

# Phase Transformation of Iron Vanadium Sulfides at High Temperatures

Hiroaki WADA

National Institute for Researches in Inorganic Materials, Namiki 1-1, Sakura-Mura, Niihari-Gun, Ibaraki 300-31

(Received March 27, 1979)

The phase relations of iron vanadium sulfides with the atomic Fe: V ratios 3: 2 and 71: 29 were examined by the high-temperature DTA and X-ray measurements. It was found that the structure of iron vanadium sulfide changes gradually from a less symmetric form to a highly symmetric form with the increase in temperature. Two types of phase transformations by vacancy order-disorder were observed at temperatures above 800 °C. One was due to the intralayer disordering of metal vacancies:  $V_3S_4$ -type  $\rightarrow$   $Cd(OH)_2$ -type (type Ia) or  $V_3S_4$ -type + NiAs-type  $\rightarrow$   $Cd(OH)_2$ -type (type Ib) at  $T_1$ . The other was due to the entirely interlayer disordering of metal vacancies:  $Cd(OH)_2$ -type  $\rightarrow$  NiAs-type (type II) at  $T_2$  ( $T_2 > T_1$ ). The tentative phase diagram of iron vanadium sulfides with the atomic Fe: V ratio 3: 2 was constructed on the basis of the DTA results.

The phase equilibrium study of a part of the Fe-V-S system has been made recently by means of thermogravimetry.<sup>1)</sup> The phase relations of the Fe-V-S system at high temperatures (500–800 °C) were presented in an earlier publication.<sup>2)</sup> From the powder X-ray diffraction patterns of the quenched specimens and the behavior of the composition-equilibrium sulfur pressure relations, it has been shown that the Fe-V-S system has extensive solid solution phases, *i.e.*,  $(Fe,V)_{1-x}S$ ,  $(Fe,V)_{3\pm x}S_4$ , and  $(Fe,V)_{5\pm x}S_8$ , which have a lattice intermediate between the NiAs-type and the  $Cd(OH)_2$ -type lattice. These phases exhibited the ordered structures of the metal vacancies due to the removal of metal atoms from every second metal layer in the fundamental NiAs-type structure, in spite of the quenching of specimens from high temperature to room temperature. This fact appears to indicate the non-quenchability of the high-temperature state, because the energy of thermal agitation promotes a state of disorder of metal vacancies with increasing temperature and the disordered phases become stable at high temperatures. Hence, it is desirable to observe the crystal structure of sulfide specimens *in situ* in order to know its real phase relations at high temperatures. However, comparatively few data have been collected on this subject with respect to iron vanadium sulfides.

The vacancy order-disorder transformation of compounds in the V-S system has been reported recently by several investigators. Nakazawa *et al.* studied a  $V_5S_8$  single crystal by means of high-temperature X-ray measurements and found that the  $V_5S_8$  phase has the intralayer order-disorder transformation at about 800 °C.<sup>3)</sup> Oka *et al.* called attention to the order-disorder transformation of the metal vacancies and determined the phase diagram of the V-S system in the compositional range from  $VS_{1.30}$  to  $VS_{1.70}$  by means of high-temperature DTA and X-ray measurements.<sup>4)</sup> Also, they explained the order-disorder transformation on the basis of statistical thermodynamic theory.<sup>5)</sup> From these reports, it is expected that compounds in the ternary system Fe-V-S have similar phase transformations at high temperatures owing to the disordering of metal vacancies.

The primary aim of this investigation was to observe the structural change of iron vanadium sulfides with temperature and to elucidate the process of its structural phase transformations. The high-temperature DTA and

X-ray measurements were employed in this study to obtain direct information on the thermal behavior and structural property of compounds. The author reports in this paper the results of high-temperature experiments of iron vanadium sulfides with the atomic Fe: V ratios 3: 2 and 71: 29.

## Experimental

**Materials and General Procedure.** The sulfide samples were synthesized by heating the mechanical mixtures of reagent grade  $VO_2 \cdot 3H_2O$  and  $FeSO_4 \cdot (NH_4)_2SO_4 \cdot 6H_2O$  in an  $H_2S$  atmosphere at 1050 °C for 4 h, and were used as starting materials. The sulfur composition of the sample was adjusted to the desired one by holding it for 5 h at the pre-determined sulfur pressure and temperature and quenching it to room temperature. The general experimental procedures, the apparatus, and the chemical analyses are the same as those described in the previous paper.<sup>1)</sup>  $Fe_{0.60}V_{0.40}S_x$  and  $Fe_{0.71}V_{0.29}S_x$ , in the compositional range of  $x=1.20$ –1.35, were used chiefly in the high-temperature experiments.

**X-Ray Study and DTA Method.** The high-temperature X-ray measurements were carried out by the film method. The X-ray powder diffraction patterns of samples were recorded at various temperatures with a precession camera ( $R=100$  mm, Mo  $K\alpha$  radiation with Zr filter). A high-power X-ray generator (Rigaku RU-200: 60 kV–200 mA) was employed for rapid measurements at high temperatures. The sulfide sample was sealed in vacuum in a silica-glass capillary (diameter 0.2 mm and thickness 0.01 mm). The capillary was mounted on a usual type of goniometer head and covered by a minifurnace with two small windows along the path of the X-ray beams. Temperature regulation was carried out up to 950 °C within the accuracy of  $\pm 5$  °C with the P.I.D control system by using a Pt–13%Rh thermocouple. The temperature of the sample was raised and kept at the desired one. The sample was exposed to X-rays for 3 h and powder photographs were taken under the conditions of 50 kV–180 mA.

The DTA measurements were carried out at the heating rate of 20 °C/min up to 1100 °C by using a Rigaku Thermo-flex DTA. About 130 mg of the sulfide powder was sealed in vacuum in a micro silica capsule specially designed for the DTA method; pure  $\alpha-Al_2O_3$  was used as the reference substance.

## Results and Discussion

**The High-temperature X-Ray Study.** The high-temperature X-ray studies were carried out in orde-

to clarify the real phase relations and the phase transformation of iron vanadium sulfide which could not be determined directly only from the thermochemical data on its composition-equilibrium sulfur pressure relations.<sup>2)</sup> Representative compounds of  $\text{Fe}_{0.60}\text{V}_{0.40}\text{S}_{1.31}$ ,  $\text{Fe}_{0.60}\text{V}_{0.40}\text{S}_{1.28}$ , and  $\text{Fe}_{0.71}\text{V}_{0.29}\text{S}_{1.20}$ , were selected for this study. Photographs were taken first at room temperature, and then at various temperatures up to 950 °C during both the heating and cooling processes.

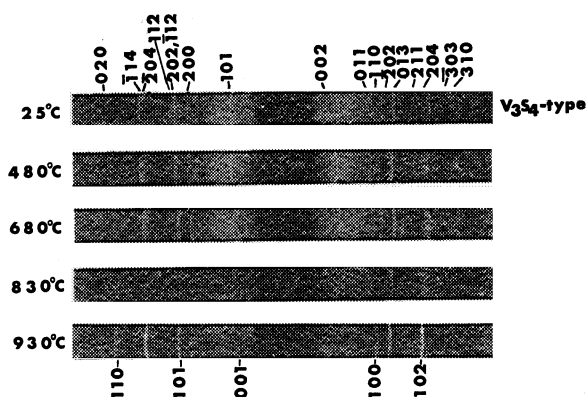


Fig. 1. The X-ray powder photographs of  $\text{Fe}_{0.60}\text{V}_{0.40}\text{S}_{1.31}$ .

Figure 1 shows a series of diffraction patterns for  $\text{Fe}_{0.60}\text{V}_{0.40}\text{S}_{1.31}$ , which has the monoclinic  $\text{V}_3\text{S}_4$ -type structure (nonreduced space group  $I2/m$  referred to the fundamental NiAs-type cell) at room temperature; its composition corresponds to that of the metal-rich phase boundary of  $(\text{Fe},\text{V})_3\text{S}_4$  solid solution at 727 °C.<sup>2)</sup>

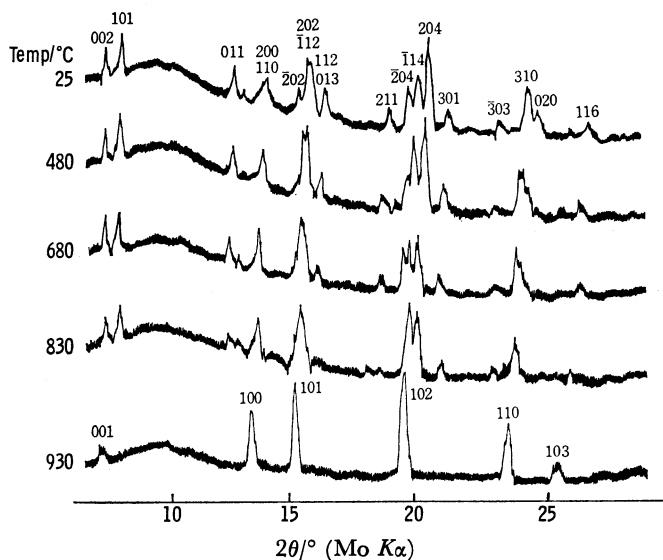


Fig. 2. The X-ray diffraction patterns of  $\text{Fe}_{0.60}\text{V}_{0.40}\text{S}_{1.31}$ .

Figure 2 gives the X-ray diffraction profiles which were reproduced from Fig. 1 by means of the micro photo-densitometer in order to represent the  $2\theta$ -intensity relations of reflections. It can be seen from these figures that the splitting of reflections which would be characteristic of the  $\text{V}_3\text{S}_4$ -type cell decreases gradually with

increasing temperature and its peak positions are shifted slightly to the lower side of  $2\theta$  values at high temperatures. This result suggests a gradual structural transformation of the monoclinic  $\text{V}_3\text{S}_4$ -type phase from a less symmetric low temperature form to a highly symmetric high temperature form. It should be emphasized that a new phase with the trigonal  $\text{Cd}(\text{OH})_2$ -type structure appears at about 930 °C. However, the high-temperature phase was not quenchable at all. On cooling the sample to room temperature, only the original patterns of  $\text{V}_3\text{S}_4$ -type was observed. This suggests that the phase transformation process of  $(\text{Fe},\text{V})_3\text{S}_4$  solid solution is reversible.

TABLE 1. THE RELATION OF THE UNIT CELL DIMENSIONS OF  $\text{Fe}_{0.60}\text{V}_{0.40}\text{S}_{1.31}$  WITH TEMPERATURE

Temp °C	$\frac{a}{\text{\AA}^b}$	$\frac{b}{\text{\AA}}$	$\frac{c}{\text{\AA}}$	$\frac{\beta}{^\circ}$	Volume $\text{\AA}^3$
25	$5.90 \pm 1$	$3.33 \pm 1$	$11.19 \pm 2$	$92.1 \pm 1$	$219 \pm 1$
480	$5.96 \pm 2$	$3.39 \pm 1$	$11.30 \pm 2$	$91.9 \pm 1$	$228 \pm 1$
680	$5.99 \pm 2$	$3.42 \pm 1$	$11.33 \pm 4$	$91.7 \pm 1$	$232 \pm 1$
830	$6.01 \pm 2$	$3.44 \pm 1$	$11.40 \pm 4$	$91.2 \pm 2$	$236 \pm 1$
930	$3.477 \pm 6^a)$		$5.738 \pm 9^a)$		$60.1 \pm 2^a)$

a) Trigonal phase. The unit cell dimensions are calculated on the basis of a  $\text{Cd}(\text{OH})_2$ -type hexagonal lattice.

b)  $\text{\AA} = 10^{-1} \text{ nm}$ .

Lattice parameters of  $\text{Fe}_{0.60}\text{V}_{0.40}\text{S}_{1.31}$  were calculated by the least-squares method<sup>6)</sup> from the data which were obtained by the film method. Temperature dependence of the unit cell dimensions is given in Table 1. It is noted that the  $a$ -,  $b$ -, and  $c$ -dimensions and the unit cell volume,  $V$ , expand linearly with the increase in temperature. On the contrary, the  $\beta$ -angle decreases gradually from 92.1 to 91.2 at temperatures between 25 and 830 °C. Also, the value of the  $c \cdot \sin \beta / 2b$  ratio, which corresponds to the  $c/a$  ratio in the NiAs-type structure, decreases from 1.68 to 1.65 in the temperature range from 25 to 930 °C. This indicates that the interlayer spacing is reduced relative to the intralayer spacing with increasing temperature, due to the difference of the directional character of the structure in the thermal expansion. In this connection, the relative expansion coefficients ( $\alpha_a = 1/a_{25^\circ\text{C}} \cdot da/dT$  and analogously for  $\alpha_b$  and  $\alpha_c$ ) were calculated from the linear relations of the unit cell dimensions with temperature. It was found that  $\alpha_a$ ,  $\alpha_b$ , and  $\alpha_c$ , and the volume expansion coefficient,  $\beta$ , are  $24 \times 10^{-6} \text{ K}^{-1}$ ,  $41 \times 10^{-6} \text{ K}^{-1}$ ,  $22 \times 10^{-6} \text{ K}^{-1}$ , and  $95 \times 10^{-6} \text{ K}^{-1}$ , respectively.

A few remarks should be made here regarding the process of the phase transformation of a  $\text{V}_3\text{S}_4$ -type cell. A possible model of the structural transformation process is shown schematically in Fig. 3. The crystal structure of the monoclinic  $\text{V}_3\text{S}_4$ -type is characterized by the ordered arrangement of metal vacancies which are confined to the alternate metal layers in the fundamental NiAs-type structure.<sup>7)</sup> This vacancy-ordered phase is stable at lower temperatures. As the temperature is raised, the energy of thermal agitation gradually increases the degree of disorder. The ordered arrangement of vacancies within the metal-deficient layer

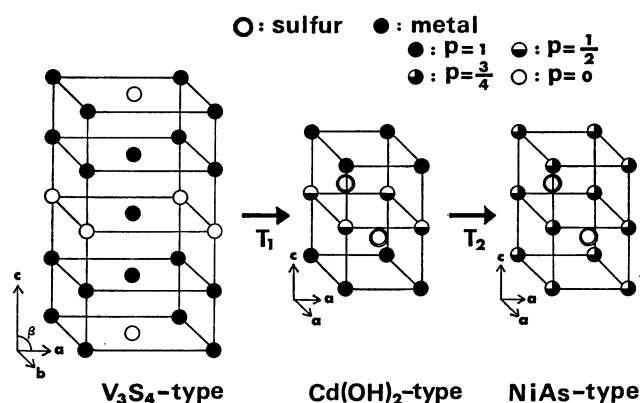


Fig. 3. A schematic model of the structural transformation of the V<sub>3</sub>S<sub>4</sub>-type phase with  $a \approx \sqrt{3} \cdot a_{\text{NiAs}}$ ;  $b \approx a_{\text{NiAs}}$ ;  $c \approx 2c_{\text{NiAs}}$ ;  $\beta \approx 92^\circ$ . Hexagonal array of sulfur is omitted in a picture of the V<sub>3</sub>S<sub>4</sub>-type structure for convenience. Symbol p denotes the occupation probability of a metal atom for each site.

changes to the entirely disordered one of the solid solution at high temperatures. A trigonal Cd(OH)<sub>2</sub>-type phase with the complete intralayer disordering becomes stable at temperatures above  $T_1$ . Further temperature elevation promotes the successive phase transformation from a trigonal Cd(OH)<sub>2</sub>-type to a hexagonal NiAs-type, based on the complete intra- and inter-layers disordering. A nonstoichiometric NiAs-type phase appears at temperatures above  $T_2$ . The schematic model of a disordering process of metal vacancies, however, may need some modifications because both the intra- and inter-layers disordering take place concomitantly with increasing temperature.<sup>3)</sup> As shown in Fig. 2, the intensity of the (001) reflection of a trigonal

TABLE 2. VARIATION OF  $d$ -SPACINGS WITH TEMPERATURE

$hkl$	$d_{\text{obsd}}/\text{\AA}$					
	25 °C	500 °C	730 °C	800 °C	850 °C	900 °C
002	5.65	5.69	5.70	5.71	5.74	5.77
101	5.17	5.19	5.26	5.28	5.30	
011	3.20	3.24	3.26	3.28	3.27	
103	3.12	3.15	3.17			
100 <sup>a)</sup>	3.00	3.04	3.06	3.06	3.05	3.04
200, 110	2.90	2.94	2.97	2.99		
$\bar{2}02$	2.60	2.68	2.70	2.70	2.68	2.69
112	2.58	2.62	2.64	2.65		
013	2.51	2.53	2.55	2.55	2.56	
211	2.15	2.17	2.20	2.20	2.21	
$\bar{2}04$	2.08	2.09	2.09	2.09	2.09	2.09
$\bar{1}14$	2.04	2.06	2.08	2.05	2.06	
204	2.00	2.02	2.04			
301	1.93	1.94	1.96	1.96	1.97	
$\bar{3}03$	1.77	1.78	1.79	1.79		
110 <sup>a)</sup>	1.73	1.76	1.76	1.76	1.75	1.75
310	1.69	1.71	1.73	1.73	1.73	
020	1.66	1.69	1.71	1.72		
116	1.57	1.58	1.59	1.60	1.62	1.62

a) (100) and (110) reflections are referred to the hexagonal NiAs-type structure.

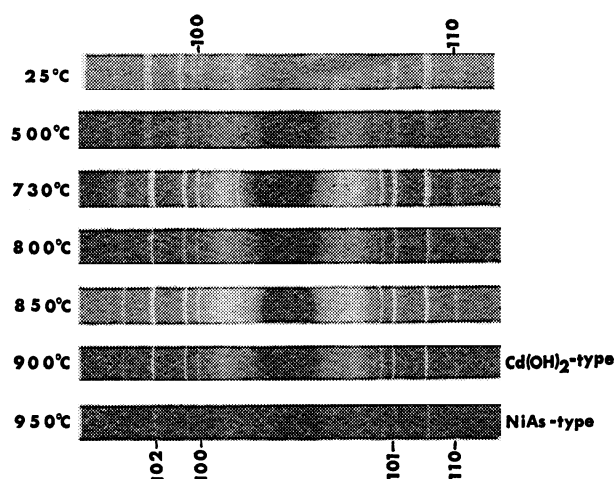


Fig. 4. The X-ray powder photographs of Fe<sub>0.60</sub>V<sub>0.40</sub>S<sub>1.28</sub>.

phase is very weak compared with that of the corresponding (002) reflection of the ordered V<sub>3</sub>S<sub>4</sub>-type phase. This may be indicative of some degree of the interlayer disordering in the process of the phase transformation.

Figure 4 shows a series of the high-temperature X-ray diffraction patterns of Fe<sub>0.60</sub>V<sub>0.40</sub>S<sub>1.28</sub>. The temperature dependence of  $d$ -spacings is listed in Table 2. The X-ray powder photograph taken at room temperature indicates clearly the presence of two phases, which are composed of (Fe,V)<sub>1-x</sub>S with hexagonal NiAs-type structure and (Fe,V)<sub>3</sub>S<sub>4</sub> with the monoclinic V<sub>3</sub>S<sub>4</sub>-type structure. However, both phases show very similar X-ray diffraction patterns, so that some reflections overlap each other. The former could be distinguished from the latter only by the presence of (100) and (110) reflections, referred to the hexagonal structure.

On heating the sample up to 850 °C, the splitting of reflections which are attributed to the V<sub>3</sub>S<sub>4</sub>-type structure gradually decreases, but the two phases still coexist. However, mutual solubility of both phases increases with increasing temperature. A new solid solution phase is formed due to the reaction of two phases at temperatures above 850 °C. The phase described above has a trigonal Cd(OH)<sub>2</sub>-type structure with intralayer disordering. Again, on heating the sample up to 950 °C, the trigonal phase transforms perfectly to the high-temperature phase with the hexagonal NiAs-type structure. This phase transformation is reversible. The trigonal phase decomposed to the original two different phases on quenching below 850 °C, owing to the phase separation.

Figure 5 shows the results of the high-temperature X-ray study of Fe<sub>0.71</sub>V<sub>0.29</sub>S<sub>1.20</sub>, which is composed of a two-phase mixture of (Fe,V)<sub>1-x</sub>S and (Fe,V)<sub>3</sub>S<sub>4</sub> at room

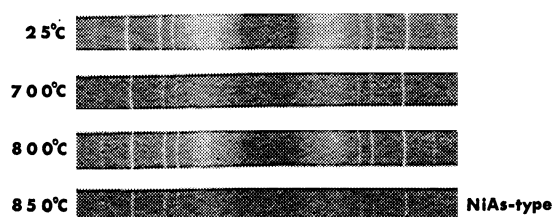


Fig. 5. The X-ray powder photographs of Fe<sub>0.71</sub>V<sub>0.29</sub>S<sub>1.20</sub>.

temperature. The intensity of the super-structure reflections derived from the  $(\text{Fe,V})_3\text{S}_4$  phase decreases gradually with increasing temperature. Finally, a high-temperature phase with the hexagonal NiAs-type structure appears at about 850 °C. However, the trigonal phase with the complete intralayer disordering could not be observed in the process of this phase transformation. This may suggest that the occurrence of the trigonal phase at high temperatures is affected by the bulk concentration of metal vacancies in the original low-temperature phases.

**The High-temperature DTA Measurement.** In order to determine the temperature of the phase transformation accurately, the DTA measurements were carried out in the temperature range from 25 to 1100 °C. Iron vanadium sulfides with the atomic Fe: V ratios 3: 2 and 71: 29 were used chiefly for the comparison with the results of the high-temperature X-ray experiments.

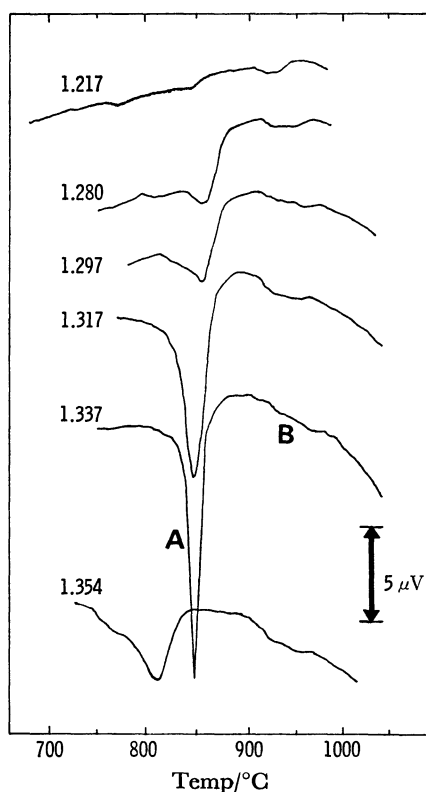


Fig. 6. DTA curves for  $\text{Fe}_{0.60}\text{V}_{0.40}\text{S}_x$ .

Figure 6 shows representative differential heating curves obtained with the composition  $\text{Fe}_{0.60}\text{V}_{0.40}\text{S}_x$ , where  $x$  lies in the range from 1.217 to 1.354. It is evident that each heating curve has two endothermic peaks in the temperature range from 700 to 1000 °C. As shown in Fig. 6, the lower one, A, is large and rather sharp in shape. On the other hand, the higher one, B, is small and broad. Note that the profile of the endothermic peaks varies clearly with the composition of sulfides. The sharpest and largest peak is observed at 842 °C in the heating curve of the composition  $x=1.337$ , which is close to the stoichiometric composition,  $(\text{Fe}_{0.60}\text{V}_{0.40})_3\text{S}_4$ . The A peak for the compositions on the sides more rich in metal than  $x=1.333$  becomes

broader and smaller with decreasing sulfur content. Also, the heating curve of the composition  $x=1.354$  shows the tendency for the A peak to grow broader and to be shifted significantly to the low temperature side with increasing sulfur content that characterizes the thermal behavior of the composition on the side more rich in sulfur than  $x=1.333$ . On the other hand, the B peaks exhibit essentially similar profiles for all of the composition studied and observed at temperatures above 900 °C.

By the direct comparison with the results of the high-temperature X-ray experiments, it is concluded that: (1) the A peak is related to the phase transformations, such as  $\text{V}_3\text{S}_4$ -type  $\rightarrow$   $\text{Cd}(\text{OH})_2$ -type (type Ia) and  $\text{V}_3\text{S}_4$ -type + NiAs-type  $\rightarrow$   $\text{Cd}(\text{OH})_2$ -type (type Ib), at the temperature  $T_1$ , and (2) the B peak is related to the phase transformation from  $\text{Cd}(\text{OH})_2$ -type to NiAs-type (type II) at the temperature  $T_2$ . The tentative phase diagram of iron vanadium sulfides with the atomic Fe: V ratio 3: 2 is shown in Fig. 7, where the tempera-

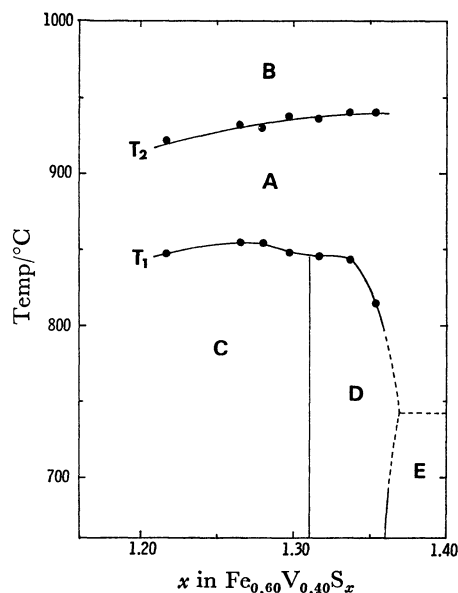


Fig. 7. Tentative phase diagram of a part of the Fe-V-S system at section with atomic Fe: V ratio 3: 2. Phase relations are represented as follows.

A:  $(\text{Fe}_{0.60}\text{V}_{0.40})_{1-x}\text{S}$  ( $\text{Cd}(\text{OH})_2$ -type),

B:  $(\text{Fe}_{0.60}\text{V}_{0.40})_{1-x}\text{S}$  (NiAs-type),

C:  $(\text{Fe,V})_{1-x}\text{S}$  (NiAs-type) +  $(\text{Fe,V})_{3\pm x}\text{S}_4$  ( $\text{V}_3\text{S}_4$ -type),

D:  $(\text{Fe}_{0.60}\text{V}_{0.40})_{3\pm x}\text{S}_4$  ( $\text{V}_3\text{S}_4$ -type),

E:  $(\text{Fe,V})_{3\pm x}\text{S}_4$  ( $\text{V}_3\text{S}_4$ -type) +  $\text{FeS}_2$  (pyrite).

The phase boundary between A and E is determined on the basis of the stability limit of pyrite.<sup>8)</sup>

tures ( $T_1$  and  $T_2$ ) at which maxima were observed on the heating curves are plotted against composition. The transformation temperature,  $T_1$ , of type Ia is connected smoothly to that of type Ib. The phase boundary curve which was determined by the  $T_1$  values has the maximum temperature of 854 °C at the composition near  $x=1.27$ . A rapid decrease of the temperature  $T_1$  is observed at the compositions on the sulfur-rich side of  $x=1.333$ . For example,  $T_1$  is about 813 °C at  $x=1.354$ . Such a compositional

dependence of  $T_1$ , as mentioned above, is similar to that of the V-S system which has been reported by Oka *et al.*<sup>4)</sup> As shown in Fig. 7, the transformation temperature  $T_2$  of the type II increases slightly with increasing sulfur content. The  $T_2$  changes from 920 to 940 °C in the compositional range of  $x=1.217-1.354$ . However, the  $T_2$  value is quite ambiguous because of the broadness of the B peak, as shown in Fig. 6.

The profiles on the differential heating curves of  $\text{Fe}_{0.71}\text{V}_{0.29}\text{S}_x$  was essentially the same as those of  $\text{Fe}_{0.60}\text{V}_{0.40}\text{S}_x$ , except that the phase transformation took place at lower temperatures. The  $T_1$  and  $T_2$  of  $\text{Fe}_{0.71}\text{V}_{0.29}\text{S}_{1.30}$  are 820 °C and 910 °C, respectively. The  $T_1$  of  $\text{Fe}_{0.71}\text{V}_{0.29}\text{S}_{1.20}$  is about 770 °C. These temperatures are relatively lower than those of the corresponding composition of  $\text{Fe}_{0.60}\text{V}_{0.40}\text{S}_x$ . According to Oka *et al.*, the  $T_1$  of  $\text{VS}_{1.33}$  is about 1200 °C.<sup>4)</sup> This temperature is much higher than that of  $\text{Fe}_{0.60}\text{V}_{0.40}\text{S}_{1.337}$  (about 840 °C). From these facts, it can be concluded that the temperature of the phase transformation of iron vanadium sulfides decreases with increasing Fe content, when the S/(Fe+V) ratio is held constant.

The author wishes to express his thanks to Professor

Mitsuoki Nakahira of Okayama College of Science for his encouragement and helpful discussion throughout this study. Thanks are also due to Dr. Hiromoto Nakazawa for his invaluable discussion, and to Drs. Akihiko Nukui and Mamoru Watanabe for their technical assistance with the high-temperature X-ray measurements during this work.

## References

- 1) H. Wada, *Bull. Chem. Soc. Jpn.*, **51**, 1368 (1978).
- 2) H. Wada, *Bull. Chem. Soc. Jpn.*, **52**, 2130 (1979).
- 3) H. Nakazawa, M. Saeki, and M. Nakahira, *Less Common Metals*, **40**, 57 (1975).
- 4) Y. Oka, K. Kosuge, and S. Kachi, *J. Solid State Chem.* **23**, 11 (1978).
- 5) Y. Oka, K. Kosuge, and S. Kachi, *J. Solid State Chem.* **24**, 41 (1978).
- 6) Computer program written by T. Sakurai, Institute of Physical and Chemical Research, Tokyo.
- 7) M. Cheverton and A. Sapet, *C. R. Acad. Sci., Paris*, **261**, 928 (1965).
- 8) G. Kullerud and H. S. Yoder, *Economic Geology*, **54**, 533 (1959).